Research Article | Vol. 26, No. 22 | 29 Oct 2018 | OPTICS EXPRESS 29159
Optics EXPRESS

Connecting two Gaussian cluster states by quantum entanglement swapping

CAIXING TIAN,[1,2] DONGMEI HAN,[1,2] YU WANG,[3,4] AND XIAOLONG SU[1,2,*]

[1]*State Key Laboratory of Quantum Optics and Quantum Optics Devices, Institute of Opto-Electronics, Shanxi University, Taiyuan, 030006, China*
[2]*Collaborative Innovation Center of Extreme Optics, Shanxi University, Taiyuan,Shanxi 030006, China*
[3]*State Key Laboratory of Cryptology, Beijing, 100878, China*
[4]*wangy@sklc.org*
[*]*suxl@sxu.edu.cn*

Abstract: Cluster state is an important resource for one-way quantum computation and quantum network. In this paper, we present a scheme for connecting two Gaussian cluster states by entanglement swapping, which can be used to connect two local quantum networks composed by cluster states. The connection schemes between different types of four-mode cluster states are analyzed and we show that the structure of the output states after entanglement swapping may be not the same as that of the input states. The entanglement of the obtained new cluster states are presented when suitable feedforward schemes are applied in the entanglement swapping process. By using optimal gains in the classical channel and inseparability criteria, the requirement of squeezing parameters for obtaining entanglement of output states are reduced. The presented scheme provides a concrete reference for constructing quantum networks with cluster states.

1. Introduction

Cluster state, a type of multipartite entangled states, is a basic quantum resource for one-way quantum computation [1]. Continuous variable (CV) cluster state [2–4], which can be generated deterministically, have been successfully produced for eight-qumode [5], 60-qumode [6] and up to 10,000-qumode [7]. Based on a prepared large scale cluster state, one-way quantum computation can be implemented by measurement and feedforward of the measurement results [8–14]. Besides the application in one-way quantum computation, cluster state can also be used to establish quantum network [15–17].

It has been demonstrated that a local quantum network can be built by distributing a multipartite entangled state among quantum nodes [18–21]. However, if we have two space-separated local quantum networks built respectively by two independent cluster states, how can we establish entanglement between these two local quantum networks? The shaping of a larger cluster state to a smaller scale according to the requirement for one-way quantum computation has been demonstrated [22]. It has also been proposed that a large scale cluster state can be generated by the fusion of small scale cluster states, which is completed by means of linear optical elements [23]. Another feasible method of merging two multipartite entangled states into one larger multipartite entangled state is the quantum entanglement swapping [24], which has been proposed to build a global quantum network of clocks. The proposed quantum clock network may allow the construction of a real-time single international time scale (world clock) with unprecedented stability and accuracy [25].

Quantum entanglement swapping is also known as quantum teleportation of entangled states [26], which makes two independent quantum entangled states become entangled, and it is an important technique in building quantum communication networks [26–36]. It was originally proposed and demonstrated in discrete-variable optical systems [27, 28], and then it was extended

#345141 https://doi.org/10.1364/OE.26.029159
Journal © 2018 Received 6 Sep 2018; revised 6 Oct 2018; accepted 6 Oct 2018; published 24 Oct 2018

Optics EXPRESS

to CV systems [26, 33–36]. Entanglement swapping between discrete and continuous variable systems has also been demonstrated [37], which shows the power of hybrid quantum information processing [38]. The entanglement swapping among three two-photon Einstein-Podolsky-Rosen (EPR) entangled states has been used to generate a Greenberger-Horne-Zeilinger (GHZ) state [39]. Also, the quantum entanglement swapping between two independent multipartite entangled states, each of which involves a tripartite GHZ entangled state of an optical field, and that between a tripartite GHZ state and an EPR entangled state have both been experimentally demonstrated [40]. Recently, the swapping schemes for EPR steering have also been proposed [41, 42].

In this paper, we present the entanglement swapping schemes between two independent CV Gaussian cluster states with different structures. By designing suitable feedforward schemes, we show that the entanglement swapping scheme between two symmetrical square shape cluster states, and that between a linear and a star-shape four-mode cluster state, can be implemented respectively. The results show that the structure of the output cluster state can be changed after the entanglement swapping, for example, the structure of output cluster state is different from that of input cluster states after the entanglement swapping between two square shape cluster states. The dependence of output entanglement in the presented entanglement swapping schemes on the squeezing parameters are analyzed, which shows that the requirement of squeezing parameter can be reduced by using the optimal gains in the classical feedforward circuits and the inseparability criteria. The presented entanglement swapping schemes have a potential application in building global quantum networks.

2. The entanglement swapping schemes

Two multipartite entangled states, A and B, consisting of m and n optical modes respectively, can be used to build two space-separated independent local quantum networks. We have shown that two space-separated independent multipartite Gaussian GHZ states can be merged into a larger multipartite entangled state by means of entanglement swapping [40]. In order to establish entanglement between the two multipartite entangled states, optical mode $\hat{A}_1$ is sent to the multipartite entangled state B through a quantum channel. A joint measurement on modes $\hat{A}_1$ and $\hat{B}_1$ is implemented and then the measurement results are fedforward to the remaining optical modes of state A and/or B. The feedforward schemes of measurement results in classical channels depend on the types of quantum correlation of the multipartite entangled states, which are more complex than those for the traditional entanglement swapping between two EPR entangled states. By quantum entanglement swapping, two multipartite entangled states consisting of m and n quantum modes respectively can be merged into a new larger multipartite entangled state which consists of $m + n - 2$ quantum modes, since two modes ($\hat{A}_1$ and $\hat{B}_1$) have been measured.

The quadrature correlations (so-called nullifiers) of CV cluster state are expressed by [2, 3, 12]

$$(\hat{p}_a - \sum_{b \in N_a} \hat{x}_b) \to 0, \qquad \forall \quad a \in G \tag{1}$$

where $\hat{x}_a = (\hat{a} + \hat{a}^\dagger)/2$ and $\hat{p}_a = (\hat{a} - \hat{a}^\dagger)/2i$ stand for amplitude and phase quadratures of an optical mode $\hat{a}$, respectively. The modes of $a \in G$ denote the vertices of the graph G, while the modes of $b \in N_a$ are the nearest neighbors of mode $\hat{a}$. For an ideal cluster state the left-hand side of Eq. (1) trends to zero, which stands for a simultaneous zero eigenstates of these quadrature combinations in the limit of infinite squeezing [12]. The special entanglement property of cluster state is that the quantum correlation only exists between two neighbor modes [1, 2]. One time measurement on cluster state can not destroy the entanglement totally, which means that cluster state has a strong property of entanglement persistence.

As an example, we present two entanglement swapping schemes for CV Gaussian cluster states, which are the entanglement swapping scheme between two independent four-mode square Gaussian cluster states (scheme I) and that between a four-mode linear and star-shape Gaussian

Optics EXPRESS

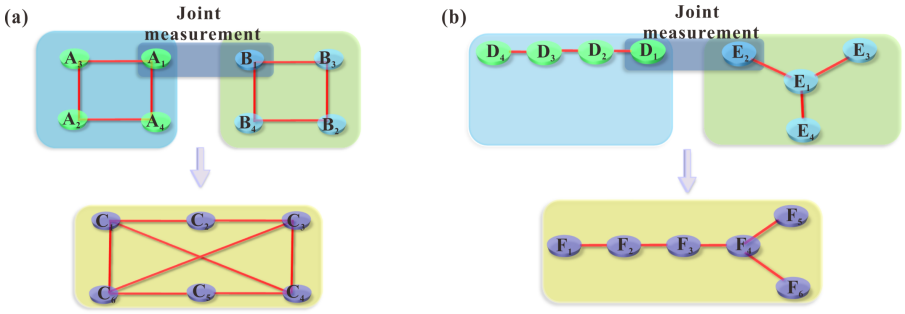

Fig. 1. Graph representation of principle for entanglement swapping between two four-mode Gaussian cluster states. Nodes and edges in the graph denote optical modes and the nearest neighbor interaction between modes. (a) The representation of entanglement swapping between two four-mode square Gaussian cluster states for scheme I. (b) The representation of entanglement swapping between a linear and a star-shape four-mode Gaussian cluster state for scheme II.

cluster states (scheme II), as shown in Fig. 1(a) and 1(b), respectively. After the entanglement swapping, a six-mode Gaussian cluster state is obtained. Please note that the structure of the output cluster states are different from those of the original Gaussian cluster states. Since the structure of the obtained six-mode Gaussian cluster states are more complicated than the four-mode Gaussian cluster states and the modes are space separated, they have potential application in quantum network for more complicated quantum communication tasks.

2.1. *Entanglement swapping between two square Gaussian cluster states*

The four-mode square Gaussian cluster state A of optical field is prepared by coupling two phase-squeezed states ($\hat{a}_1$ and $\hat{a}_4$) of light and two amplitude-squeezed states ($\hat{a}_2$ and $\hat{a}_3$) of light on an optical beam-splitter network, which consists of three optical beam-splitters with transmittance of $T_{A1} = T_{A2} = 1/5$ and $T_{A3} = 1/2$, respectively. The other four-partite square Gaussian cluster state B of optical field is prepared in the same way. The transformation matrixes of the beam-splitter networks for establishing four-partite square cluster entangled states A and B are given by

$$U_A = U_B = \begin{bmatrix} -\sqrt{\frac{1}{2}} & -\sqrt{\frac{2}{5}} & -i\sqrt{\frac{1}{10}} & 0 \\ \sqrt{\frac{1}{2}} & -\sqrt{\frac{2}{5}} & -i\sqrt{\frac{1}{10}} & 0 \\ 0 & i\sqrt{\frac{1}{10}} & \sqrt{\frac{2}{5}} & \sqrt{\frac{1}{2}} \\ 0 & i\sqrt{\frac{1}{10}} & \sqrt{\frac{2}{5}} & -\sqrt{\frac{1}{2}} \end{bmatrix}. \tag{2}$$

The unitary matrix can be decomposed into a beam-splitter network $U_A = B^+_{34}(T_{A3})F_3B^-_{12}(T_{A2})I_1(-1)I_2(-1)B^+_{23}(T_{A1})F_3$, where $F_k = e^{i\frac{\pi}{2}}$ denotes a Fourier transformation of mode k ($k = 1, 2, 3, 4$), which corresponds to a 90° rotation in the phase space; $I_k(-1) = e^{i\pi}$ corresponds to a 180° rotation in phase space; $B^{\pm}_{kl}(T_j)$ stands for the linear optical transformation on the j-th beam-splitter with transmittance of $T_{Aj(Bj)}$ ($j = 1, 2, 3$), where $\left(B^{\pm}_{kl}\right)_{kk} = \sqrt{1-T}$, $\left(B^{\pm}_{kl}\right)_{kl} = \sqrt{T}$, $\left(B^{\pm}_{kl}\right)_{lk} = \pm\sqrt{T}$, and $\left(B^{\pm}_{kl}\right)_{ll} = \mp\sqrt{1-T}$, are matrix elements of the beam-splitter. The decomposition of unitary matrix for the cluster state B is the same to that for the cluster state A.

Optics EXPRESS

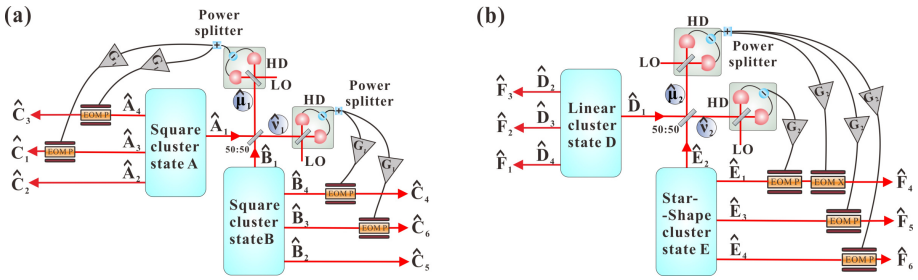

Fig. 2. Schematic of two entanglement swapping schemes. (a) Scheme for entanglement swapping between two four-mode square Gaussian cluster states. The joint measurement is performed on optical modes $\hat{A}_1$ and $\hat{B}_1$ coming from two cluster states A and B, respectively. The measurement results are fedforward to the remaining quantum modes of multipartite entangled states A and B through classical channels, respectively. (b) Scheme for entanglement swapping between a four-mode linear and a star-shape Gaussian cluster states. The joint measurement is performed on optical modes $\hat{D}_1$ and $\hat{E}_2$ coming from two multipartite entangled states D and E, respectively. The measurement results are fedforward to the remaining quantum modes of multipartite entangled state E through classical channels. EOMX and EOMP, amplitude and phase electro-optical modulators; HD, homodyne detector; LO, local beam. The power splitter is used to split the output photocurrent from the homodyne detector.

The quantum correlations of the four-mode square cluster state are given by

$$\begin{aligned}
\hat{p}_{A_1} - \hat{x}_{A_3} - \hat{x}_{A_4} &= -\sqrt{\frac{1}{2}}\hat{p}^{(0)}_{a_1}e^{-r} - \sqrt{\frac{5}{2}}\hat{x}^{(0)}_{a_3}e^{-r}, \\
\hat{p}_{A_2} - \hat{x}_{A_3} - \hat{x}_{A_4} &= \sqrt{\frac{1}{2}}\hat{p}^{(0)}_{a_1}e^{-r} - \sqrt{\frac{5}{2}}\hat{x}^{(0)}_{a_3}e^{-r}, \\
\hat{p}_{A_3} - \hat{x}_{A_1} - \hat{x}_{A_2} &= \sqrt{\frac{1}{2}}\hat{p}^{(0)}_{a_4}e^{-r} + \sqrt{\frac{5}{2}}\hat{x}^{(0)}_{a_2}e^{-r}, \\
\hat{p}_{A_4} - \hat{x}_{A_1} - \hat{x}_{A_2} &= -\sqrt{\frac{1}{2}}\hat{p}^{(0)}_{a_4}e^{-r} + \sqrt{\frac{5}{2}}\hat{x}^{(0)}_{a_2}e^{-r},
\end{aligned} \tag{3}$$

respectively, where $\hat{x}^{(0)}_{a_j}$ and $\hat{p}^{(0)}_{a_j}$ $(j = 1, 2, 3, 4)$ denote the amplitude and phase quadratures of corresponding vacuum field, respectively, and r is the squeezing parameter ($r = 0$ and $r \to \infty$ correspond to no squeezing and the ideally perfect squeezing, respectively). Obviously, in the ideal case with infinite squeezing ($r \to \infty$) these correlation variances will vanish, and the better the squeezing, the smaller the variances. Here, we only present the expressions of quantum correlations for the cluster state A since quantum correlations of the cluster state B are the same to those of the state A.

As shown in Fig. 2(a), the optical mode $\hat{A}_1$ is transmitted from multipartite entangled state A to multipartite entangled state B and mixed with $\hat{B}_1$ on a 50:50 beam-splitter with $\pi/2$ phase difference. The output modes from the beam-splitter $\hat{\mu}_1 = (\hat{A}_1 + i\hat{B}_1)/\sqrt{2}$ and $\hat{v}_1 = (\hat{A}_1 - i\hat{B}_1)/\sqrt{2}$ are measured by two homodyne detectors, respectively. The measured quadratures $\hat{x}_{\mu_1}$ and $\hat{p}_{v_1}$ are given by

$$\begin{aligned}
\hat{x}_{\mu_1} &= \frac{1}{\sqrt{2}}(\hat{x}_{A_1} - \hat{p}_{B_1}), \\
\hat{p}_{v_1} &= \frac{1}{\sqrt{2}}(\hat{p}_{A_1} - \hat{x}_{B_1}),
\end{aligned} \tag{4}$$

Optics EXPRESS

respectively. The measurement results are fedforward to optical modes $\hat{A}_3$, $\hat{A}_4$, $\hat{B}_3$ and $\hat{B}_4$ through classical channels respectively. Concretely, the measurement result of $\hat{x}_{\mu_1}$ is fedforward to $\hat{p}_{A_3}$ and $\hat{p}_{A_4}$, and $\hat{p}_{\nu_1}$ is fedforward to $\hat{p}_{B_4}$ and $\hat{p}_{B_3}$, respectively. The amplitude and phase quadratures of output state C are expressed by

$$\begin{aligned}
\hat{x}_{C_1} &= \hat{x}_{A_3}, & \hat{p}_{C_1} &= \hat{p}_{A_3} - \sqrt{2}G_1\hat{x}_{\mu_1}, \\
\hat{x}_{C_2} &= \hat{x}_{A_2}, & \hat{p}_{C_2} &= \hat{p}_{A_2}, \\
\hat{x}_{C_3} &= \hat{x}_{A_4}, & \hat{p}_{C_3} &= \hat{p}_{A_4} - \sqrt{2}G_1\hat{x}_{\mu_1}, \\
\hat{x}_{C_4} &= \hat{x}_{B_4}, & \hat{p}_{C_4} &= \hat{p}_{B_4} + \sqrt{2}G_1\hat{p}_{\nu_1}, \\
\hat{x}_{C_5} &= \hat{x}_{B_2}, & \hat{p}_{C_5} &= \hat{p}_{B_2}, \\
\hat{x}_{C_6} &= \hat{x}_{B_3}, & \hat{p}_{C_6} &= \hat{p}_{B_3} + \sqrt{2}G_1\hat{p}_{\nu_1},
\end{aligned} \tag{5}$$

respectively. The parameter G_1 describes the gain in classical channels. Without loss of generality, we assume the gain in the classical channels are the same.

The quantum entanglement among the output modes of Gaussian cluster state C is verified by the inseparability criteria for a six-mode Gaussian cluster state shown in Fig. 1(a) [43], which are

$$\Delta^2(\hat{p}_{C_1} - \hat{x}_{C_2} - g_{C_1}\hat{x}_{C_6} - g_{C_1}\hat{x}_{C_4}) + \Delta^2(\hat{p}_{C_2} - \hat{x}_{C_1} - g_{C_1}\hat{x}_{C_3}) < 1, \tag{6a}$$

$$\Delta^2(\hat{p}_{C_1} - g_{C_2}\hat{x}_{C_2} - g_{C_2}\hat{x}_{C_6} - \hat{x}_{C_4}) + \Delta^2(\hat{p}_{C_4} - g_{C_2}\hat{x}_{C_3} - g_{C_2}\hat{x}_{C_5} - \hat{x}_{C_1}) < 1, \tag{6b}$$

$$\Delta^2(\hat{p}_{C_1} - g_{C_3}\hat{x}_{C_2} - \hat{x}_{C_6} - g_{C_3}\hat{x}_{C_4}) + \Delta^2(\hat{p}_{C_6} - \hat{x}_{C_1} - g_{C_3}\hat{x}_{C_5} - g_{C_3}\hat{x}_{C_3}) < 1, \tag{6c}$$

$$\Delta^2(\hat{p}_{C_2} - g_{C_4}\hat{x}_{C_1} - \hat{x}_{C_3}) + \Delta^2(\hat{p}_{C_3} - \hat{x}_{C_2} - g_{C_4}\hat{x}_{C_4} - g_{C_4}\hat{x}_{C_6}) < 1, \tag{6d}$$

$$\Delta^2(\hat{p}_{C_3} - g_{C_5}\hat{x}_{C_2} - \hat{x}_{C_4} - g_{C_5}\hat{x}_{C_6}) + \Delta^2(\hat{p}_{C_4} - \hat{x}_{C_3} - g_{C_5}\hat{x}_{C_5} - g_{C_5}\hat{x}_{C_1}) < 1, \tag{6e}$$

$$\Delta^2(\hat{p}_{C_3} - g_{C_6}\hat{x}_{C_2} - g_{C_6}\hat{x}_{C_4} - \hat{x}_{C_6}) + \Delta^2(\hat{p}_{C_6} - g_{C_6}\hat{x}_{C_1} - g_{C_6}\hat{x}_{C_5} - \hat{x}_{C_3}) < 1, \tag{6f}$$

$$\Delta^2(\hat{p}_{C_4} - g_{C_7}\hat{x}_{C_3} - \hat{x}_{C_5} - g_{C_7}\hat{x}_{C_1}) + \Delta^2(\hat{p}_{C_5} - \hat{x}_{C_4} - g_{C_7}\hat{x}_{C_6}) < 1, \tag{6g}$$

$$\Delta^2(\hat{p}_{C_5} - g_{C_8}\hat{x}_{C_4} - \hat{x}_{C_6}) + \Delta^2(\hat{p}_{C_6} - g_{C_8}\hat{x}_{C_1} - \hat{x}_{C_5} - g_{C_8}\hat{x}_{C_3}) < 1. \tag{6h}$$

The parameter g_{C_i} $(i = 1, 2, ..., 8)$ are gain factors used to minimize the correlation variances at the left-hand sides of Eq. (6). Physically, the parameters g_{C_i} correspond to the gain in the measurement of correlation variances shown in the inseparability criteria.

By calculating the minimum values of left-hand sides of Eq. (6), we obtain a few combinations of optimal gain factors G_1 in classical channels and g_{C_i} in the inseparability criteria. Then we choose the one corresponding to the minimum requirement of squeezing parameter for success of the entanglement swapping scheme. The chosen optimal gain in the classical channels is

$$G_1 = \frac{1 - 22e^{4r} + 21e^{8r}}{11 + 68e^{4r} + 21e^{8r}}. \tag{7}$$

The calculated optimal gains g_{C_i} $(i = 1, 2, ..., 8)$ are given by

$$\begin{aligned}
g_{C_1} &= g_{C_4} = g_{C_7} = g_{C_8} = \frac{21e^{8r} - 12e^{4r} - 9}{46 + 83e^{4r} + 21e^{8r}}, \\
g_{C_2} &= g_{C_3} = g_{C_5} = g_{C_6} = \frac{21e^{8r} - 12e^{4r} - 9}{11 + 68e^{4r} + 21e^{8r}},
\end{aligned} \tag{8}$$

respectively.

Optics EXPRESS

2.2. Entanglement swapping between a linear and a star-shape Gaussian cluster states

A four-mode linear Gaussian cluster state D of optical field is prepared by coupling two phase-squeezed states ($\hat{d}_1$ and $\hat{d}_4$) of light and two amplitude-squeezed states ($\hat{d}_2$ and $\hat{d}_3$) of light on an optical beam-splitter network, which consists of three optical beam-splitters with transmittance of $T_{D1} = 1/5$, $T_{D2} = 1/2$ and $T_{D3} = 1/2$, respectively. A four-partite star-shape Gaussian cluster state E of optical field is prepared by coupling two phase-squeezed states ($\hat{e}_1$ and $\hat{e}_3$) of light and two amplitude-squeezed states ($\hat{e}_2$ and $\hat{e}_4$) of light on an optical beam-splitter network with transmittance of the beam splitters being $T_{E1} = T_{E2} = T_{E3} = 1/2$, respectively. The transformation matrixes of the beam-splitter networks for producing four-mode cluster states D and E are given by

$$U_D = \begin{bmatrix} \sqrt{\frac{1}{2}} & \sqrt{\frac{2}{5}} & i\sqrt{\frac{1}{10}} & 0 \\ i\sqrt{\frac{1}{2}} & -i\sqrt{\frac{2}{5}} & \sqrt{\frac{1}{10}} & 0 \\ 0 & \sqrt{\frac{1}{10}} & -i\sqrt{\frac{2}{5}} & i\sqrt{\frac{1}{2}} \\ 0 & i\sqrt{\frac{1}{10}} & \sqrt{\frac{2}{5}} & \sqrt{\frac{1}{2}} \end{bmatrix}, \tag{9}$$

$$U_E = \begin{bmatrix} i\sqrt{\frac{1}{2}} & -\frac{i}{2} & \frac{i}{2} & 0 \\ \sqrt{\frac{1}{2}} & \frac{1}{2} & -\frac{1}{2} & 0 \\ 0 & \frac{1}{2} & \frac{1}{2} & i\sqrt{\frac{1}{2}} \\ 0 & \frac{1}{2} & \frac{1}{2} & -i\sqrt{\frac{1}{2}} \end{bmatrix}, \tag{10}$$

respectively. The unitary matrix U_D and U_E can be decomposed into beam-splitter networks $U_D = F_4F_2B^+_{34}(T_{D3})F_4B^+_{12}(T_{D2})B^+_{23}(T_{D1})F_3$, and $U_E = F_1B^+_{34}(T_{E3})F_4B^+_{12}(T_{E2})B^-_{23}(T_{E1})I_2(-1)$, respectively. The quantum correlations of the two states are given by

$$\begin{aligned}
\hat{p}_{D_1} - \hat{x}_{D_2} &= \sqrt{2}\hat{p}^{(0)}_{d_1}e^{-r}, \\
\hat{p}_{D_2} - \hat{x}_{D_1} - \hat{x}_{D_3} &= \sqrt{\frac{1}{2}}\hat{p}^{(0)}_{d_4}e^{-r} - \sqrt{\frac{5}{2}}\hat{x}^{(0)}_{d_2}e^{-r}, \\
\hat{p}_{D_3} - \hat{x}_{D_2} - \hat{x}_{D_4} &= \sqrt{\frac{1}{2}}\hat{p}^{(0)}_{d_1}e^{-r} - \sqrt{\frac{5}{2}}\hat{x}^{(0)}_{d_3}e^{-r}, \\
\hat{p}_{D_4} - \hat{x}_{D_3} &= \sqrt{2}\hat{p}^{(0)}_{d_4}e^{-r}, \\
\hat{p}_{E_1} - \hat{x}_{E_2} - \hat{x}_{E_3} - \hat{x}_{E_4} &= -2\hat{x}^{(0)}_{e_2}e^{-r}, \\
\hat{p}_{E_2} - \hat{x}_{E_1} &= \sqrt{2}\hat{p}^{(0)}_{e_1}e^{-r}, \\
\hat{p}_{E_3} - \hat{x}_{E_1} &= \sqrt{\frac{1}{2}}\hat{p}^{(0)}_{e_1}e^{-r} + \hat{p}^{(0)}_{e_3}e^{-r} + \sqrt{\frac{1}{2}}\hat{x}^{(0)}_{e_4}e^{-r}, \\
\hat{p}_{E_4} - \hat{x}_{E_1} &= \sqrt{\frac{1}{2}}\hat{p}^{(0)}_{e_1}e^{-r} + \hat{p}^{(0)}_{e_3}e^{-r} - \sqrt{\frac{1}{2}}\hat{x}^{(0)}_{e_4}e^{-r},
\end{aligned} \tag{11}$$

respectively.

As shown in Fig. 2(b), the optical mode $\hat{D}_1$ is transmitted from multipartite entangled state D to multipartite entangled state E and mixed with $\hat{E}_2$ on a 50:50 beam-splitter with $\pi/2$ phase difference. The output modes $\hat{\mu}_2 = (\hat{D}_1 + i\hat{E}_2)/\sqrt{2}$ and $\hat{\nu}_2 = (\hat{D}_1 - i\hat{E}_2)/\sqrt{2}$ are measured by two

Optics EXPRESS

homodyne detectors, respectively. The measured quadratures $\hat{x}_{\mu_2}$ and $\hat{p}_{\nu_2}$ are given by

$$\begin{aligned} \hat{x}_{\mu_2} &= \frac{1}{\sqrt{2}}(\hat{x}_{D_1} - \hat{p}_{E_2}), \\ \hat{p}_{\nu_2} &= \frac{1}{\sqrt{2}}(\hat{p}_{D_1} - \hat{x}_{E_2}), \end{aligned} \tag{12}$$

respectively. The measurement results of $\sqrt{2}G_2(\hat{x}_{\mu_2} + \hat{p}_{\nu_2})$ are fedforward to amplitude and phase quadratures of mode $\hat{E}_1$, and $\sqrt{2}G_2\hat{x}_{\mu_2}$ is fedforward to phase quadratures of modes $\hat{E}_3$ and $\hat{E}_4$ through classical channels, respectively. The amplitude and phase quadratures of the output states are expressed by

$$\begin{aligned} \hat{x}_{F_1} &= \hat{x}_{D_4}, \qquad \hat{p}_{F_1} = \hat{p}_{D_4}, \\ \hat{x}_{F_2} &= \hat{x}_{D_3}, \qquad \hat{p}_{F_2} = \hat{p}_{D_3}, \\ \hat{x}_{F_3} &= \hat{x}_{D_2}, \qquad \hat{p}_{F_3} = \hat{p}_{D_2}, \\ \hat{x}_{F_4} &= \hat{x}_{E_1} + \sqrt{2}G_2\hat{x}_{\mu_2}, \\ \hat{p}_{F_4} &= \hat{p}_{E_1} + \sqrt{2}G_2\hat{p}_{\nu_2}, \\ \hat{x}_{F_5} &= \hat{x}_{E_3}, \qquad \hat{p}_{F_5} = \hat{p}_{E_3} + \sqrt{2}G_2\hat{x}_{\mu_2}, \\ \hat{x}_{F_6} &= \hat{x}_{E_4}, \qquad \hat{p}_{F_6} = \hat{p}_{E_4} + \sqrt{2}G_2\hat{x}_{\mu_2}, \end{aligned} \tag{13}$$

respectively. The parameter G_2 describes the gain in the classical channels.

The quantum entanglement among the output modes in multipartite entangled state F is verified by the inseparability criteria for a six-mode Gaussian cluster state shown in Fig. 1(b) [43], which are

$$\Delta^2(\hat{p}_{F_1} - \hat{x}_{F_2}) + \Delta^2(\hat{p}_{F_2} - \hat{x}_{F_1} - g_{F_1}\hat{x}_{F_3}) < 1, \tag{14a}$$

$$\Delta^2(\hat{p}_{F_2} - g_{F_2}\hat{x}_{F_1} - \hat{x}_{F_3}) + \Delta^2(\hat{p}_{F_3} - \hat{x}_{F_2} - g_{F_2}\hat{x}_{F_4}) < 1, \tag{14b}$$

$$\Delta^2(\hat{p}_{F_3} - g_{F_3}\hat{x}_{F_2} - \hat{x}_{F_4}) + \Delta^2(\hat{p}_{F_4} - \hat{x}_{F_3} - g_{F_3}\hat{x}_{F_5} - g_{F_3}\hat{x}_{F_6}) < 1, \tag{14c}$$

$$\Delta^2(\hat{p}_{F_4} - g_{F_4}\hat{x}_{F_3} - \hat{x}_{F_5} - g_{F_4}\hat{x}_{F_6}) + \Delta^2(\hat{p}_{F_5} - \hat{x}_{F_4}) < 1, \tag{14d}$$

$$\Delta^2(\hat{p}_{F_4} - g_{F_5}\hat{x}_{F_3} - g_{F_5}\hat{x}_{F_5} - \hat{x}_{F_6}) + \Delta^2(\hat{p}_{F_6} - \hat{x}_{F_4}) < 1. \tag{14e}$$

Where the optimal gain in the classical channels is

$$G_2 = \frac{17e^{4r} - 17}{17e^{4r} + 23}. \tag{15}$$

The calculated optimal gains g_{F_i} $(i = 1, 2, ..., 6)$ are given by

$$\begin{aligned} g_{F_1} &= \frac{2e^{4r} - 2}{3 + 2e^{4r}}, \\ g_{F_2} &= \frac{3(e^{4r} - 1)(3 + 17e^{4r})}{81 + 68e^{4r} + 51e^{8r}}, \\ g_{F_3} &= \frac{7(e^{4r} - 1)(3 + 17e^{4r})}{(8 + 7e^{4r})(23 + 17e^{4r})}, \\ g_{F_4} &= g_{F_5} = \frac{(e^{4r} - 1)(9 + 391e^{4r})}{(23 + 17e^{4r})(17 + 23e^{4r})}, \end{aligned} \tag{16}$$

respectively.

Optics EXPRESS

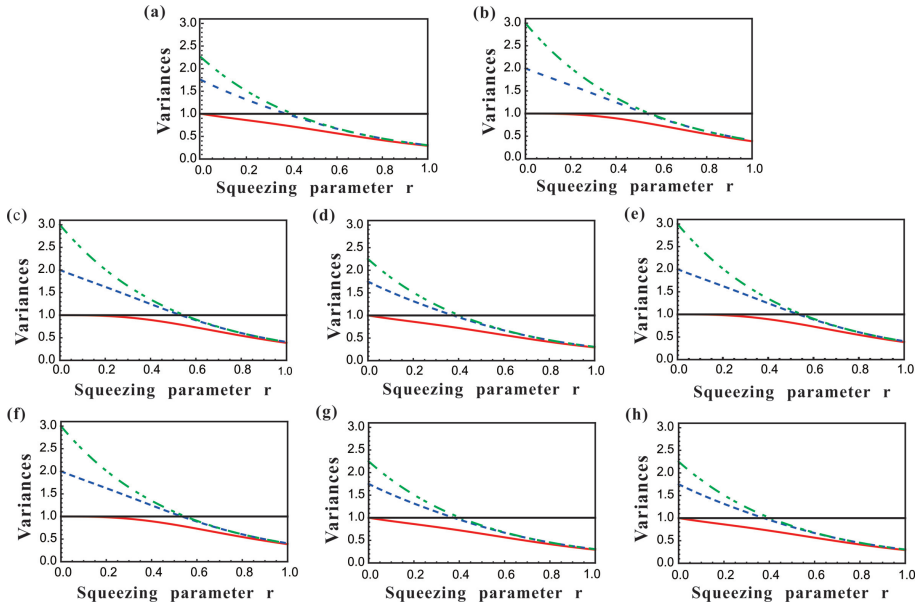

Fig. 3. The inseparability criteria for the obtained six-mode cluster entangled state in entanglement swapping scheme I. (a) - (h) are corresponding to (a) - (h) inequalities in Eq. (6), respectively. Green dash-dotted lines and blue dashed lines represent the results with unit and optimal gain G_1 in classical channels, respectively, when the unit gains g_{C_i} in the inseparability criteria are chosen. Red solid lines represent the results with both optimal gains G_1 and g_{C_i}.

3. Results and discussion

The entanglement of output state after entanglement swapping depends on squeezing parameter of the initial CV entangled states since the entanglement of CV system is related to the squeezing parameter. The higher squeezing parameter is, the higher entanglement is. Fig. 3 shows the dependence of inseparability criteria of the output six-mode cluster state on squeezing parameter for entanglement swapping scheme I. The gain in classical channels is an essential experimental parameter in CV entanglement swapping [26, 34, 35]. We compare the inseparability criteria of the output six-mode cluster state with different gain G_1 in classical channels and gains g_{C_i} ($i = 1, 2, ..., 8$) in Eq. (6). If the gains G_1 in classical channels and gains g_{C_i} ($i = 1, 2, ..., 8$) in the inseparability criteria are all chosen to be unit, the output state is entangled only when the squeezing parameter is higher than 0.55 [−4.78 dB squeezing, green dash-dotted lines in Figs. 3(b), 3(c), 3(e) and 3(f)]. If the gain G_1 in classical channels is optimal, and the unit gain g_{C_i} ($i = 1, 2, ..., 8$) is chosen, the output state is entangled when the squeezing parameter is higher than 0.53 [−4.60 dB squeezing, blue dashed lines in Figs. 3(b), 3(c), 3(e) and 3(f)]. However, when optimal gain factors G_1 [Eq. (7)] and g_{C_i} ($i = 1, 2, ..., 8$) [Eq. (8)] are both used, the requirement of entanglement on the squeezing parameter is reduced to 0 (red solid lines). The left-hand sides of Eq. (6) are all smaller than 1 and thus demonstrate the success of entanglement swapping between two square cluster states.

Fig. 4 shows the dependence of inseparability criteria of the output six-mode cluster state on squeezing parameter for entanglement swapping scheme II. The gain in classical channels and gains g_{F_i} ($i = 1, 2, ..., 5$) in the inseparability criteria are also used to optimize the output

Optics EXPRESS

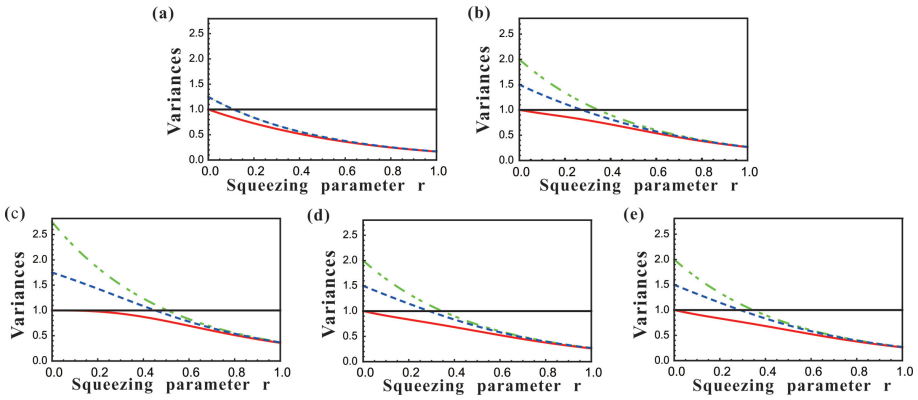

Fig. 4. The inseparability criteria for the obtained six-mode cluster entangled state in swapping scheme II. (a) - (e) are corresponding to (a) - (e) inequalities in Eq. (14), respectively. Green dash-dotted lines and blue dashed lines represent the results with unit and optimal gain G_2 in classical channels, respectively, when the unit gains g_{F_i} in the inseparability criteria are chosen. Red solid lines represent the results with both optimal gains G_2 and g_{F_i}.

entanglement in the entanglement swapping scheme II. When the gains g_{F_i} $(i = 1, 2, ..., 5)$ in the inseparability is unit, the left-hand side of inequality (14a) is the same for the case that the gain G_2 in classical channels is unit and optimal, as shown in Fig. 4(a). This is because the left-hand side of inequality (14a) is not related to the gain G_2 in classical channels. We can also see that the optimal gain factors G_2 [Eq. (15)] and g_{F_i} [Eq. (16)] are helpful to reduce the requirement of squeezing parameter (red solid lines).

The presented entanglement swapping scheme of CV cluster state is different from that of CV GHZ state in [40]. At first, the feedforward schemes in classical channels are different. In the entanglement swapping of multipartite entangled state, the feedforward scheme in classical channels depends on the quantum correlation type of the state. In the entanglement swapping of CV GHZ state, the measurement results are only fedforward to one CV GHZ state (for example, state B in [40]). While in the presented entanglement swapping scheme I, the measurement results are fedforward to optical modes in both cluster states A and B. Secondly, the output states after entanglement swapping are different. In the entanglement swapping of CV GHZ state, the output state is still CV GHZ state. While in the presented entanglement swapping of CV Gaussian cluster state, the output state is CV Gaussian cluster state and the structure of the output state may not the same as the initial cluster state.

4. Conclusion

In summary, we proposed feasible schemes for entanglement swapping between two independent Gaussian cluster states. Two specific entanglement swapping schemes between two four-mode Gaussian cluster states with different structures are presented. After entanglement swapping, two independent four-mode Gaussian cluster states are merged into a six-mode Gaussian cluster state. We find that the structure of the output Gaussian cluster state may be different from the initial Gaussian cluster states. The dependence of output entanglement on squeezing parameter for different types of Gaussian cluster states are analyzed. The results show that the requirement on squeezing can be reduced by using optimal gains in the classical channels and entanglement criterion.

Optics EXPRESS

Since a local quantum network can be established by distributing optical modes of a cluster state to different quantum nodes, the presented scheme can be used to merge two space-separated local quantum networks composed by Gaussian cluster states into a larger quantum network. The presented results provide a concrete reference for constructing more complicated quantum networks with Gaussian cluster states.

Funding

This research was supported by National Natural Science Foundation of China (Grants No. 11522433, No. 11504024, No. 61475092, and No. 11834010); the program of Youth Sanjin Scholar; National Key R&D Program of China (Grant No. 2016YFA0301402); and the Fund for Shanxi "1331 Project" Key Subjects Construction.

References

1. H. J. Briegel and R. Raussendorf, "Persistent entanglement in arrays of interacting particles," Phys. Rev. Lett. **86,** 910-913 (2001).
2. J. Zhang and S. L. Braunstein, "Continuous-variable Gaussian analog of cluster states," Phys. Rev. A **73,** 032318 (2006).
3. P. van Loock, C. Woodbrook, and M. Gu, "Building Gaussian cluster states by linear optics," Phys. Rev. A **76**, 032321 (2007).
4. N. C. Menicucci, S. T. Flammia, and P. van Loock,"Quantifying entanglement of arbitrary-dimensional multipartite pure states in terms of the singular values of coefficient matrices," Phys. Rev. A **83**, 042335 (2011).
5. X. Su, Y. Zhao, S. Hao, X. Jia, X. Jia, C. Xie, and K. Peng, "Experimental preparation of eight-partite cluster state for photonic qumodes," Opt. Lett. **37**, 5178-5180 (2012).
6. M. Chen, N. C. Menicucci, and O. Pfister, "Experimental realization of multipartite entanglement of 60 modes of a quantum optical frequency comb," Phys. Rev. Lett. **112**, 120505 (2014).
7. S. Yokoyama, R. Ukai, S. C. Armstrong, C. Sornphiphatphong, T. Kaji, S. Suzuki, J.-i. Yoshikawa, H. Yonezawa, N. C. Menicucci, and A. Furusawa, "Ultra-large-scale continuous-variable cluster states multiplexed in the time domain," Nature Photon. **7**, 982-986 (2013).
8. R. Raussendorf and H. J. Briegel, "A one-way quantum computer," Phys. Rev. Lett. **86,** 5188-5191 (2001).
9. P. Walther, K. J. Resch, T. Rudolph, E. Schenck, H. Weinfurter, V. Vedral, M. Aspelmeyer, and A. Zeilinger, "Experimental one-way quantum computing," Nature **434**, 169–176 (2005).
10. N. C. Menicucci, P. van Loock, M. Gu, C. Weedbrook, T. C. Ralph, and M. A. Nielsen, Phys. Rev. Lett. **97,** "Universal quantum computation with continuous-variable cluster states," 110501 (2006).
11. P. van Loock, "Examples of Gaussian cluster computation," J. Opt. Soc. Am. B. **24**, 340–346 (2007).
12. M. Gu, C. Weedbrook, N. C. Menicucci, T. C. Ralph, and P. van Loock, "Quantum computing with continuous-variable clusters," Phys. Rev. A **79**, 062318 (2009).
13. R. Ukai, N. Iwata, Y. Shimokawa, S. C. Armstrong, A. Politi, J. I. Yoshikawa, P. van Loock, and A. Furusawa, "Demonstration of unconditional one-way quantum computations for continuous variables," Phys. Rev. Lett. **106,** 240504 (2011).
14. X. Su, S. Hao, X. Deng, L. Ma, M. Wang, X. Jia, C. Xie, and K. Peng, "Gate sequence for continuous variable one-way quantum computation," Nat. Commun. **4,** 2828 (2013).
15. H. Shen, X. Su, X. Jia, and C. Xie, "Quantum communication network utilizing quadripartite entangled states of optical field," Phys. Rev. A **80,** 042320 (2009).
16. H.-K. Lau and C. Weedbrook, "Quantum secret sharing with continuous-variable cluster states," Phys. Rev. A **88,** 042313 (2013).
17. X. Deng, Y. Xiang, C. Tian, G. Adesso, Q. He, Q. Gong, X. Su, C. Xie and K. Peng, "Demonstration of monogamy relations for Einstein-Podolsky-Rosen steering in Gaussian cluster states," Phys. Rev. Lett. **118,** 230501 (2017).
18. P. van Loock and S. L. Braunstein, "Multipartite entanglement for continuous variables: a quantum teleportation network," Phys. Rev. Lett. **84,** 3482-3485 (2000).
19. H. Yonezawa, T. Aoki, and A. Furusawa, "Demonstration of a quantum teleportation network for continues variables," Nature (London) **431,** 430-433 (2004).
20. J. Jing, J. Zhang, Y. Yan, F. Zhao, C. Xie, and K. Peng, "Experimental demonstration of tripartite entanglement and controlled dense coding for continuous variables," Phys. Rev. Lett. **90,** 167903 (2003).
21. J. Roslund, R. M. de Araújo, S. Jiang, C. Fabre, and N. Treps, "Wavelength-multiplexed quantum networks with ultrafast frequency combs," Nat. Photon. **8,** 109-112 (2013).
22. Y. Miwa, R. Ukai, J.-I. Yoshikawa, R. Filip, P. van Loock, and A. Furusawa, "Demonstration of cluster-state shaping and quantum erasure for continuous variables," Phys. Rev. A **82,** 032305 (2010).
23. D. E. Browne and T. Rudolph, "Resource-efficient linear optical quantum computation," Phys. Rev. Lett. **95,** 010501 (2005).

Optics EXPRESS

24. S. Bose, V. Vedral, and P. L. Knight, "Multiparticle generalization of entanglement swapping," Phys. Rev. A **57,** 822-829 (1998).
25. P. Kómár, E. M. Kessler, M. Bishof, L. Jiang, A. S. Sørensen, J. Ye, and M. D. Lukin, "A quantum network of clocks," Nat. Phys. **10,** 582-587 (2014).
26. P. van Loock and S. L. Braunstein, "Unconditional teleportation of continuous-variable entanglement," Phys. Rev. A **61,** 010302 (1999).
27. M. Żukowski, A. Zeilinger, M. A. Horne, and A. K. Ekert, "Event-ready-detectors" Bell experiment via entanglement swapping," Phys. Rev. Lett. **71,** 4287-4290 (1993).
28. J.-W. Pan, D. Bouwmeester, H. Weinfurter, and A. Zeilinger, "Experimental entanglement swapping: entangling photons that never interacted," Phys. Rev. Lett. **80,** 3891-3894 (1998).
29. F. Sciarrino, E. Lombardi, G. Milani, and F. De Martini, "Delayed-choice entanglement swapping with vacuum–one-photon quantum states," Phys. Rev. A **66,** 024309 (2002).
30. H. de Riedmatten, I. Marcikic, J. A. W. van Houwelingen, W. Tittel, H. Zbinden, and N. Gisin, "Long-distance entanglement swapping with photons from separated sources," Phys. Rev. A **71,** 050302 (2005).
31. Y.-B. Sheng, F.-G. Deng and G. Long, "Complete hyperentangled-Bell-state analysis for quantum communication, " Phys. Rev. A **82,** 032318 (2010).
32. L. Zhou and Y.-B. Sheng, "Complete logic Bell-state analysis assisted with photonic Faraday rotation, " Phys. Rev. A **92,** 042314 (2015).
33. R. E. S. Polkinghorne and T. C. Ralph, "Continuous variable entanglement swapping," Phys. Rev. Lett. **83**, 2095-2099 (1999).
34. S. M. Tan, "Confirming entanglement in continuous variable quantum teleportation,"Phys. Rev. A **60,** 2752-2758 (1999).
35. X. Jia, X. Su, Q. Pan, J. Gao, C. Xie, and K. Peng, "Experimental demonstration of unconditional entanglement swapping for continuous variables," Phys. Rev. Lett. **93,** 250503 (2004).
36. N. Takei, H. Yonezawa, T. Aoki, and A. Furusawa, "High-fidelity teleportation beyond the no-cloning limit and entanglement swapping for continuous variables," Phys. Rev. Lett. **94,** 220502 (2005).
37. S. Takeda, M. Fuwa, P. van Loock, and A. Furusawa, "Entanglement swapping between discrete and continuous variables," Phys. Rev. Lett. **114,** 100501 (2015).
38. U. L. Andersen, J. S. Neergaard-Nielsen, P. van Loock, and A. Furusawa, "Hybrid discrete- and continuous-variable quantum information," Nat. Phys. **11,** 713-719 (2015).
39. C.-Y. Lu, T. Yang, and J.-W. Pan, "Experimental multiparticle entanglement swapping for quantum networking," Phys. Rev. Lett. **103,** 020501 (2009).
40. X. Su, C. Tian, X. Deng, Q. Li, C. Xie, and K. Peng, "Quantum entanglement swapping between two multipartite entangled states," Phys. Rev. Lett. **117,** 240503 (2016).
41. M. Wang, Z. Qin and X. Su, "Swapping of Gaussian Einstein-Podolsky-Rosen steering," Phys. Rev. A **95**, 052311 (2017).
42. M. Wang, Z. Qin, Y. Wang and X. Su, "Einstein-Podolsky-Rosen-steering swapping between two Gaussian multipartite entangled states," Phys. Rev. A **96**, 022307 (2017).
43. P. van Loock, and A. Furusawa, "Detecting genuine multipartite continuous-variable entanglement," Phys. Rev. A **67**, 052315 (2003).